Journal of Applied Electrochemistry **30**: 107–111, 2000.

Short communication

Preparation and characterization of microporous Ni coatings as hydrogen evolving cathodes

I.J. BROWN and S. SOTIROPOULOS
School of Chemical, Environmental and Mining Engineering, Nottingham University, University Park, Nottingham NG7 2RD, Great Britain

Received 12 April 1999; accepted in revised form 29 June 1999

Key words: hydrogen evolving cathodes, microporous Ni coatings, microporous polymers

1. Introduction

A number of industrial electrochemical processes employ high surface area Ni electrodes. These include the use of Ni anodes in alkaline or molten carbonate fuel cells [1–3], NiO(OH) cathodes in nickel–cadmium and nickel–hydrogen batteries [4] and hydrogen evolving Ni cathodes in alkaline water electrolysis [5] as well as in electrochemical hydrogenation of organics [6]. There are various types of high surface area Ni electrodes and an even larger variety of preparation methods. Sintered microporous Ni coatings are usually manufactured according to the ceramic foil-casting technology, by mixing of a micrometer size nickel powder with an organic binder, which is subsequently thermally decomposed with further sintering at elevated temperatures in a hydrogen atmosphere [3]. The methods for the production of nanoporous Raney–Ni coatings include cold rolling, plasma spraying, annealing, sherardizing and cathodic codeposition of the Raney–nickel precursor alloys (Ni/Al or Ni/Zn) on a nickel support [7].

PolyHIPE Polymer (PHP) [8, 9] is a microporous material produced through the formation of a high internal phase water-in-oil emulsion, in which the volume of the aqueous dispersed phase is greater than about 75%, and the subsequent polymerization (at 60 °C) of the oil phase which contains the monomer (styrene and occasionally other monomers too) and the cross-linker (divinylbenzene). This results in the production of a porous polymer matrix due to the evaporation of the water droplets, which were present in the precursor emulsion. The structure of PHP is characterized by the presence of numerous cells (of 1–100 μm diameter) interconnected by smaller pores (of 0.1–10 μm diameter).We have recently reported the incorporation of Ni into the PHP matrix by electroplating through its pores and onto a thin Au layer electrode pasted on one side of a polymer sample [10] or onto a Ni mesh in a Ni/PHP/Ni composite cell [11]. Thermal decomposition of the polymer resulted in a granular Ni structure of BET surface areas in the range of 1–50 $m^2\ g^{-1}$ depending on the method and plating current density. The main advantages of this process for producing nickel coatings of morphology comparable to that of sintered Ni are the inexpensive raw materials for the polymer matrix production and the relatively low temperature processing. Furthermore, the high surface area coating can be deposited on a variety of substrate electrode materials (e.g., stainless steel, reticulated vitreous carbon) and on substrates of different geometries. The work presented here introduces a further modification of the technique, whereby only the Ni cathode wire is immersed into the precursor emulsion and finally entrapped into a well-defined PHP coating after polymerization. A preliminary characterization of the porous Ni coating, produced after electroplating and polymer decomposition, with respect to hydrogen evolution from alkaline solutions is also presented.

2. Experimental details

2.1. *Preparation of Ni/PHP composite electrodes*

Polymer of an 80% void was produced by using 80% v/v aqueous phase in the precursor water-in-oil emulsion. The composition of the oil phase was (by volume): 15% styrene (Aldrich, 99%), 62% 2-ethylhexyl-acrylate (Aldrich), 8% divinylbenzene (Aldrich, 80%) and 15% sorbitan monooleate (Aldrich, 95%). The aqueous phase was distilled water and 1% w/w potassium persulphate (Aldrich, 99% +) which acted as the polymerization initiator. The emulsion was produced by careful mixing according to a procedure described elsewhere [10, 11] and then poured into 3 mm diameter glass tubes. A 1 mm thick Ni wire cathode (99.99%, Goodfellow Ltd) was suspended from the top with the help of a small clamp and immersed in the emulsion in the centre of the tube. Polymerization was performed for 6 h in an oven heated at 60 °C and subsequent drying and cleaning followed [10, 11]. The Ni/PHP composite cathode thus prepared, together with the cylindrical Ni mesh anode

(26×26 wires per inch 0.25 mm thick, Goodfellow Ltd), is shown schematically in Figure 1.

2.2. *Ni electroplating and polymer decomposition*

A standard nickel sulphamate bath [12] served as the electroplating solution at 60 °C: 600 g dm^{-3} nickel sulphamate (Aldrich, 98%), 10 g dm^{-3} nickel chloride (Aldrich) and 40 g dm^{-3} boric acid (Aldrich, 99.5% +). A Radiometer Voltalab® 21 potentiostat/galvanostat was used to carry out the electroplating at 10 mA cm^{-2} of Ni wire geometric area. Prior to electroplating the Ni/PHP electrode was activated by immersion into a 1:1 HCl–water solution for a few minutes. The burnout of the polymeric matrix of the Ni/PHP composites after electroplating was carried out under an air atmosphere in a preheated furnace at 500 °C, for 1 h. SEM and EDAX analysis of the resulting material have confirmed complete polymer burnout at the end of this procedure [24]. SEM experiments on the Ni-coated electrodes were carried out with a Hitachi S-570 SEM. Prior to electrochemical experiments the electrodes were further treated in a 20% H_2O_2 solution for 30 min (to oxidise organic residual impurities) and briefly (30 s) immersed in a 1:1 conc. HCl–water solution followed by thorough rinsing with ultrapure water.

2.3. *Electrochemistry of Ni-coated electrodes*

A three-electrode cell with a Pt coil counter electrode (BAS Technicol Ltd) and a saturated calomel electrode (SCE, EG&G) equiped with a salt bridge ending to a Vycor® tip (EG&G), were used. Potentiodynamic and potentiostatic experiments were performed with an Autolab 30 potentiostat (Eco Chemie BV, Windsor Scientific Ltd) using current-interrupt *IR* compensation. Solutions of NaOH were prepared using sodium hydroxide pellets (99.98%, Aldrich) and all experiments were carried out at 20 °C.

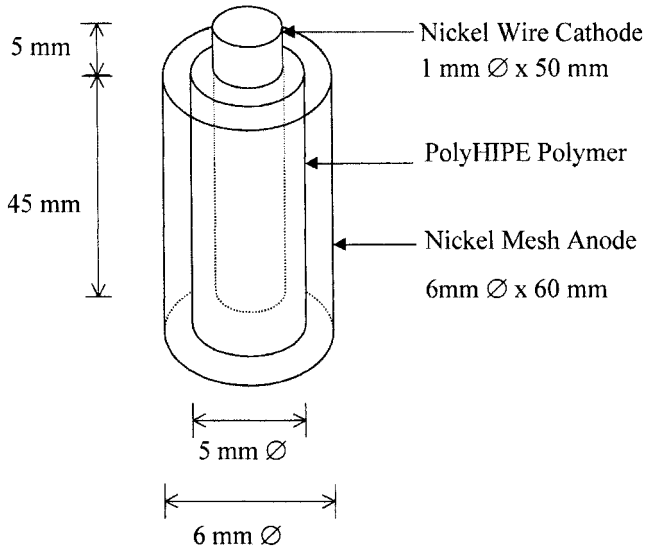

Fig. 1. Ni/PHP composite cathode surrounded by a cylindrical Ni mesh anode in a typical electroplating arrangement.

3. Results and discussion

3.1. *Ni electrodeposits*

Figure 2(a) shows the SEM micrograph of PolyHIPE polymer before plating and a regular structure of closed but porous cells can be seen. In more detail, the polymer structure consists of large cells of a 10–30 μm diameter, corresponding to the water droplets of the initial water-in-oil emulsion, interconnected by smaller pores of a 3–5 μm diameter, which correspond to the contact areas of

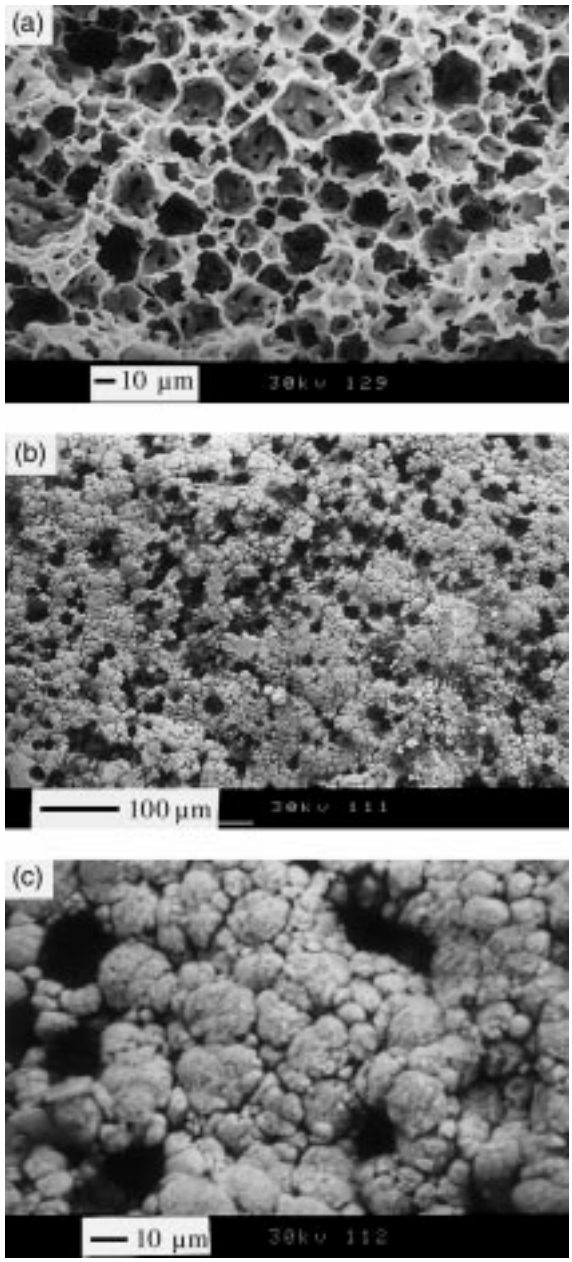

Fig. 2. (a) SEM micrograph of a PolyHIPE polymer (PHP) sample at a 350× magnification; (b) SEM micrograph of a porous Ni coating on a Ni wire at a 160× magnification; (c) SEM micrograph of the Ni coating of the previous micrograph at a 800× magnification.

the initially present water droplets. Figure 2(b) shows the structure of the Ni electrodeposit formed onto the Ni cathode wire after electroplating for 24 h at a rate of 10 mA cm^{-2} and subsequent polymer decomposition. It can be seen that a uniform microporous Ni coating has been produced onto the substrate consisting of spherical agglomerates and voids. Figure 2(c) is an SEM micrograph of the same deposit at higher magnifications showing the prevalence of large near-spherical agglomerates 5–20 μm in diameter and fewer voids of similar dimensions. The larger of the agglomerates correspond to partially filled polymer cells. They are themselves made up of smaller aggregates and are linked to each other by even smaller Ni particles, the latter corresponding to Ni growing through the polymer pores. Although there is no straightforward host–guest relationship between the polymer matrix and the metal deposit (this should have led to simple spherical aggregates of 10–30 μm size filling completely the polymer void), it is certainly the distortion of the electric field due to the insulating PHP shield during plating, that gives the Ni deposit its structure. For an electrodeposit growing through a locally structured matrix local current densities will vary significantly from pore to pore and from cell to cell [13]. The deposition will preferentially proceed around already plated pores rather than around new pores of the same cell. Once an entire cell is filled with Ni, deposition will preferentially start in a neighbouring cell closer to the anode than in one lying at the same plane with the Ni-filled cell. These effects will lead to either partially filled or completely void polymer cells in accordance with Figure 2(b) and (c). By weighing the wire before and after plating the plating current efficiency was determined to be 99% in accordance with the literature [14].

From the thickness of the coating (700 μm; diameter of the Ni-coated wire as measured by SEM and a micrometer was 2.4 mm and that of the plain wire 1 mm), an estimate of the porosity of the coating was made as follows. The volume of a hypothetical concentric nonporous 700 μm thick deposit around a 1 mm diameter wire can be calculated to be 0.037 cm^3 per cm of wire. The mass of nickel deposited around the wire was measured as 0.129 g per cm of wire, corresponding to 0.015 cm^3 Ni per cm of wire. Therefore, the porosity of the deposit is approximately 60%.

3.2. *Electrochemistry of porous Ni coatings*

Figure 3(a) shows the cyclic voltammogram at 50 mV s^{-1} of a Ni-coated electrode in 0.5 M NaOH in the potential region that a monolayer of α-$Ni(OH)_2$ is formed/stripped off [15, 16], whereas Figure 3(b) shows a similar voltammogram recorded at a polished Ni disc electrode. In the latter, the peaks correspond to the oxidation of Ni to α-$Ni(OH)_2$ (anodic peak at -0.7 V vs SCE) and the reduction of the latter upon potential reversal (cathodic peak at -1.1 V vs SCE), as reported in the literature [15, 16]. In the case of the Ni-coated

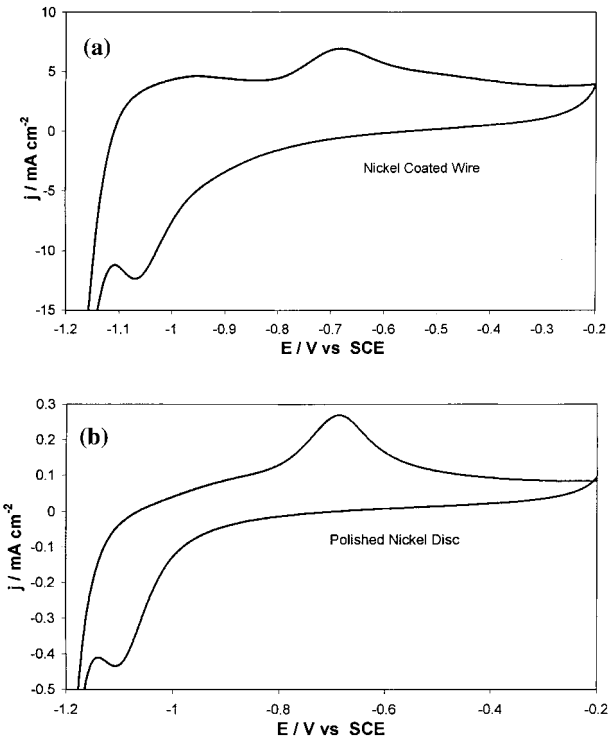

Fig. 3. (a) Voltammogram recorded at a porous Ni coating on a Ni wire in a deaerated 0.5 M NaOH solution at a potential scan rate of 50 mV s^{-1}; (b) same as before but for a smooth Ni disc electrode.

electrode these peaks are less defined since they are expected to be affected by higher charging currents, a situation already documented for high surface area Ni electrodes [17, 18]. The charge associated with the formation/reduction of a monolayer of α-$Ni(OH)_2$ is known to be 514 μC cm^{-2} [15–17] and estimation of the area under the cathodic peak gives a roughness factor (ratio of true to geometric area) of 1.3 for the smooth Ni disc and 83 for the Ni-coating. Table 1 presents the values of the roughness factor for the Ni disc and Ni coating, as well as the relative increase in true area.

Figure 4(a) presents the potential sequence applied to the Ni-coated electrode during the potentiostatic experiments performed to obtain near steady-state current–potential data. The Ni-coated electrode was cathodised at a potential of -1.6 V vs SCE in the hydrogen evolution region for over 1 h before commencing the potentiostatic experiment and 5 min between applying the potential pulses. For each reading the potential of the Ni-coated electrode was switched between -1.021 and -1.2 V vs SCE for 1 min before switching to the potential of interest and the current collected after 2 min. Similar sequences are recommended for reproducible surface state of Ni during steady state polarization measurements [16, 20]. Figure 4(b) presents the semi-logarithmic *IE* curves obtained from these experiments. A Tafel slope of 120 mV $decade^{-1}$ was recorded for smooth Ni, in accordance with the prevalence of the Volmer–Heyrovski mechanism [16, 20]. A slope of 120 mV $decade^{-1}$ was also found for the Ni-coated electrodes, in accordance with data for sintered Ni that

Table 1. Relative true areas and Tafel slopes for smooth and Ni-coated Ni electrodes

	Roughness factor $r/cm^2\ cm^{-2}$	Relative true area based on r	Normalized current density at $\eta = 0.3$ V j/mA cm^{-2}		Tafel slope /mV dec^{-1}
			True area	Geometric area	
Smooth Ni	1.3	1	1.1	1.4	120
Ni-coated Ni	83	64	1.2	100	120

appear in the literature [7] and in contrast to the much lower values reported for Raney–Ni [7, 17, 19]. In Table 1, the current per true (electroactive) and geometric electrode area is given for both smooth and Ni-coated electrodes for $\eta = 0.3$ V. The fact that the Tafel slope remains the same as one passes from smooth to these porous Ni electrodes and that the hydrogen evolution apparent current density (i.e., current per geometric electrode area) at the latter is enhanced by a factor of 100:1.4 (=71.5) which is comparable to the increase of 83:1.3 (=64) in the true area, indicates that the superior performance of the porous coating is not due to a change in the mechanism but to an increase in the electroactive area.

The situation prevailing at our microporous coatings is different from that observed at nanoporous Raney–Ni coatings, nanostructured Ni–metal codeposited alloys and fine-structured porous coatings in general. For those coatings a change of the reaction mechanism with decreasing current density has been reported and two regions of different Tafel slopes have been found. In more detail, the extremely high roughness factors (1000–10000) encountered at Raney–Ni and Ni–metal alloy electrodes makes regimes of very low true current densities accessible and in these regimes the rate determining step for hydrogen evolution is an electrochemical desorption step resulting in a low value of about 40 mV $decade^{-1}$, in contrast to the 120 mV $decade^{-1}$ observed at high current densities [21]. In our porous coatings of rather low roughness factors (of the order of 100), only the high (true) current density region is accessible and hence a high Tafel slope is observed. In theoretical work by Bockris and Srinivasan [22] an increase of Tafel slope values by a factor of up to two is attributed to ohmic losses within fine-structured porous coatings. However, our coatings have a very open structure (porosity of about 60%), a thickness that does not exceed 1 mm and the uncompensated resistance, measured by the current interrupt technique, was found to be as low as 3–6 Ω. This indicates that ohmic effects cannot affect the I/E behaviour of the system especially after *IR* correction has been carried out. Table 2 presents a comparison of the hydrogen evolution overpotentials encountered at 100 mA cm^{-2} with our electrodes and with some indicative sintered Ni [7] and Raney–Ni [7, 19] electrodes reported in the literature. It can be seen that the performance of our Ni-coated electrode is at least comparable to that of sintered Ni electrodes.

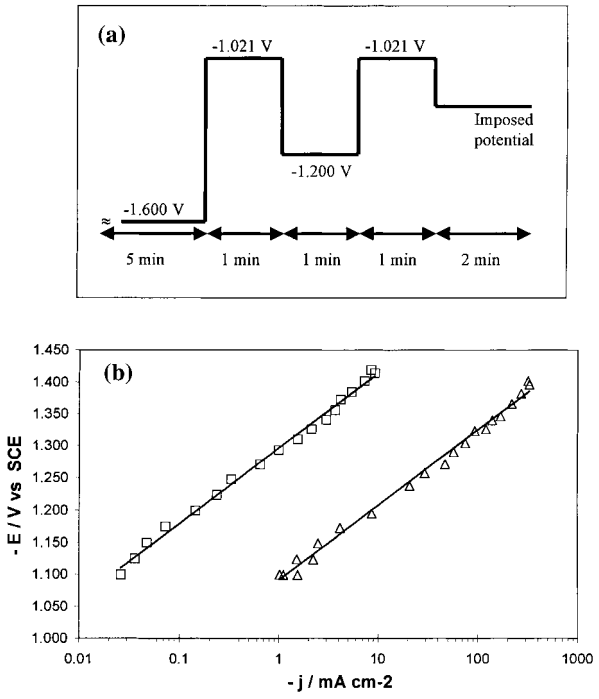

Fig. 4. (a) Potential sequence for electrode activation during collection of steady state polarization data; (b) Tafel plots for hydrogen evolution at smooth (□) and porous (△) Ni-coated electrodes.

4. Conclusion

A new preparation method for microporous Ni coatings on electrodes has been established. Ni is electroplated through the pores of a generic microporous polymer coating onto the cathode and subsequent polymer thermal decomposition results in a porous Ni coating. These cathodes showed promising current densities for hydrogen evolution, in the range of those encountered at sintered Ni coatings. The microporous coatings introduced here involve the thermal decomposition of a polymer, in a manner similar to the first steps in the preparation of sintered Ni electrode coatings which also involve the decomposition of a binder [3]. However, they

Table 2. Overpotentials for hydrogen evolution at indicative Ni cathodes, at 100 mA cm^{-2} (geometric) current density

	Porous Ni coating This work	Sintered Ni coating [7]	Smooth Raney–Ni [7]	Electrodeposited Ni–Zn [19]
$\eta_{100\ mA\ cm^{-2}}$/mV	300	360	240	150

do not require the high temperature processing (sintering in reducing atmosphere) needed in the production of sintered Ni.

We are currently investigating the electrochemical behaviour of Ni coatings prepared from Ni/PHP electrodes at higher current densities since preliminary experiments [12] indicated a change in the deposit morphology and the appearance of submicrometer needles. We are also investigating other low temperature alternatives for removing the emulsion or polymer matrix after electroplating, without the need for thermal decomposition.

Acknowledgements

The authors wish to thank EPSRC for a studentship to I.J.B, the University of Nottingham for a New Lecturers' Research Grant and the Royal Society for a Research Grant to S.S.

References

1. T.C. Benjamin, E.H. Camera and L.G. Marianowski, *in* 'Handbook of Fuel Cells', Institute of Gas Technology, Chicago (1980).
2. S. Ye, A.K. Vijh and L.H. Dao, *J. Electrochem. Soc.* **144** (1997) 90.
3. O. Böhme, F.U. Leidich, H.J. Salge and H. Wendt, *Int. J. Hydrogen Energy* **19** (1994) 349.
4. C.A. Vincent and B. Scrosati, 'Modern Batteries', 2nd edn (Arnold, London, 1997).
5. K. Wall, 'Modern Chlor–Alkali Technology', Vol. 3 (Ellis Horwood, Chichester, 1986).
6. V. Anantharaman and P.N. Pintauro, *J. Electrochem. Soc.* **141** (1994) 2729.
7. S. Rausch and H. Wendt, *J. Electrochem. Soc.* **143** (9) (1996) 2852.
8. D. Barby and Z. Haq, *European Patent 0 060 138* assigned to Unilever (1982).
9. J. Williams, *Langmuir* **4** (1988) 44.
10. S. Sotiropoulos, I.J. Brown, G. Akay and E. Lester, *Materi. Lett.* **35** (1998) 383.
11. I.J. Brown, D. Clift and S. Sotiropoulos, *Materi. Res. Bull.* to appear in **34** (7), (1999).
12. F.A. Lowenheim, *in* 'Electroplating' (McGraw-Hill, New York 1978).
13. L. Cai and H.Y. Cheh, Meeting Abstracts of the 191st Meeting of The Electrochemical Society Inc., Abstract 51, Montreal (1997), p. 58.
14. A.K. Graham, 'Electroplating Engineering Handbook', (Van Nostrand, 1971), p. 248.
15. F. Hahn, B. Beden, M.J. Croissant and C. Lamy, *Electrochim. Acta* **31** (3) (1986) 335.
16. S.A.S. Machado and L.A. Avaca, *Electrochim. Acta* **39** (10) (1994) 1385.
17. B.E. Conway and L. Bai, *J. Chem. Soc. Faraday Trans. I* **81** (1985) 1841.
18. E.A. Ticianelli, C.R. Derouin and S. Srinivasan, *J. Electroanal. Chem.* **251** (1988) 275.
19. M.J. De Giz, S.A.S. Machado, L.A. Avaca and E.R. Conzalez, *J. Appl. Electrochem.* **22** (1992) 973.
20. A.N. Correia and S.A.S. Machado, *Electrochim. Acta* **43**(3–4) (1998) 367.
21. R.P. Simpraga and B.E. Conway, *Electrochim. Acta* **43**(19–20) (1998) 3045.
22. J.O'M. Bockris and S. Srinivasan, 'Fuel Cells: Their Electrochemistry' (McGraw-Hill, New York, 1969).